Catalysis Today 367 (2021) 258–267

Contents lists available at ScienceDirect

Catalysis Today

journal homepage: www.elsevier.com/locate/cattod

Methyl ketones from carboxylic acids as valuable target molecules in the biorefinery

Olivier Marie [a], Alexey V. Ignatchenko [b], Michael Renz [c,*]

[a] Normandie Univ., ENSICAEN, UNICAEN, CNRS, LCS, 14000, Caen, France
[b] Chemistry Department, St. John Fisher College, 3690 East Avenue, Rochester, NY 14618, USA
[c] Instituto de Tecnología Química, Universitat Politècnica de Valencia – Consejo Superior de Investigaciones Científicas (UPV-CSIC), Avda. de los Naranjos s/n, 46022, Valencia, Spain

ARTICLE INFO

Keywords:
Carbon atom efficiency
DFT calculation
e-factor
Isotopic labeling
In-situ IR spectroscopy
Operando IR spectroscopy

ABSTRACT

For the preparation of methyl ketones, cross Ketonic Decarboxylation, i.e., the formation of a ketone from two different carboxylic acids, and the reketonization, i.e., the transformation of a carboxylic acid into a ketone employing a ketone as alkyl transfer agent, may be interesting alternatives to classical pathways involving metal-organic reagents.

The fine chemical 2-undecanone was chosen as model compound and ketonic decarboxylation and reketonization evaluated by Green Chemistry matrices, namely the carbon atom efficiency and the e-factor. The e-factor of the reaction of decanoic acid with acetic acid was less than five and, therewith, in the acceptable range for bulk chemicals, when valorizing acetone (e.g., as a solvent) and considering a 90% solvent recycling. The reketonization of decanoic acid with acetone provided a different main product, namely 10-nonadecanone, with a detrimental effect on atom efficiency.

By means of labeling experiments it was shown that ketonic decarboxylation is significantly faster than the reketonization reaction. The transformation of acetic acid into acetone was studied by *in-situ* and *operando* IR spectroscopy. Thereby it was found that the surface was covered by acetic acid. The lack of adsorption of acetone is a clear drawback for the reketonization of carboxylic acids. To improve the reaction outcome, and therewith, its sustainability a possibility has to be found to stabilize the ketone molecules on the surface in the presence of carboxylic acids.

1. Introduction

Methyl ketones are interesting fine chemicals. Methyl ethyl ketone (MEK, butanone) and methyl isobutyl ketone (MIBK, 4-methyl-2-pentanone) are employed as solvents for paints, coatings, adhesives, inks and other applications [1]. Several methyl ketones with a longer, linear second-alkyl chain such as 2-heptanone, 2-octanone, 2-nonanone, 2-undecanone, and 2-tridecanone are commercialized in the fragrance and flavor industry [2]. In addition, 2-undecanone is applied as an insect and animal repellant [3–5].

Applying classical Organic Chemistry, methyl ketones may be produced by the means of metalorganic reagents such as Grignard reagents, reacting carboxylic acid esters with MeMgBr. However, this reaction does not stop at the ketone stage, but goes further to the tertiary alcohol due to double addition of the Grignard reagent [6–11]. To avoid the transformation of the intermediary ketone, a special technique has to be employed: the Weinreb ketone synthesis. In a first step, an amide with N, O-dimethylhydroxylamine has to be prepared that allows only a single addition of the Grignard reagent [12–16]. Such a synthesis pathway is thus possible, but tedious and, in addition, Grignard reagents are not welcome in chemical industry. Special safety requirements have to be adopted due to their reactivity.

The ketonic decarboxylation of two carboxylic acid molecules into a ketone can be considered as an alternative pathway [17]. Thereby, the cross-coupling version with acetic acid and any carboxylic acid leads to methyl ketones. From the two different reactants, three products are obtained: the two homo-coupling products (acetone and a symmetrical ketone involving a longer alkyl chain) and the cross-coupling product (methyl ketone). Therefore, the maximum selectivity towards the methyl ketone is 50% for statistical reasons when the two carboxylic

* Corresponding author.
E-mail address: mrenz@itq.upv.es (M. Renz).

https://doi.org/10.1016/j.cattod.2020.03.042
Received 26 December 2019; Received in revised form 13 March 2020; Accepted 20 March 2020
Available online 27 March 2020

acids are employed in a one to one molar ratio.

It should be noted that neither one of the two extreme cases – exclusive formation of an unsymmetrical ketone, or a mixture of two symmetrical ketones - have been reported in literature. Some acids, which do not have alpha protons, such as pivalic, benzoic acid, etc., are not able to enolize. Therefore, such acids cannot form symmetrical ketones and they are spent entirely for the preparation of a methyl ketone in their reaction with acetic acid. The problem of the cross-ketone selectivity dependence on the ratio of two acids as well as on the type of metal oxide catalyst has been studied in details [18]. Both positive and negative deviations from statistically expected values for the selectivity towards methyl *iso*-propyl ketone from a mixture of acetic and isobutyric acids have been found.

For the reaction between a mixture of two enolizable acids, the selectivity to one of the symmetrical ketones can be reduced while the selectivity to the cross-ketone, such as methyl ketone, can be increased on a purely statistical basis by using an excess of the second acid. From the economical point of view, it may make sense to carry out the reaction with an excess of acetic acid. In general, this carboxylic acid is much cheaper than the higher homologue. Then, the formation of the long chain ketone is suppressed and the formation of the cross-coupling product, i.e., the methyl ketone, is increased together with that of acetone. If only the long-chain carboxylic acid is taken into account for the calculation of the yield, and the acetic acid considered a reactant employed in excess, the yield of the methyl ketone can be significantly increased. The penalty for the improved yield is the coproduction of acetone in excess. This is a clear disadvantage from the sustainability point of view.

A second alternative to produce methyl ketones consists in reacting acetone with carboxylic acids (Eq. (1) and (2)). This reaction has been first reported in the patent literature in 1989 and recently rediscovered [19,20]. The reaction sequence has been described postulating a 1, 3-diketone as key intermediate (Eq. (2)) and the sequence named "reketonization". In the first step, acetone is acylated to produce the 1, 3-diketone. The latter compounds are known to be prone to cleavage reactions. Hence, surface hydroxyl groups assist this transformation and form part of an adsorbed carboxylate product after the reaction. The selectivity of the decomposition of the diketone is governed by thermodynamic means: the more stable products, i.e., the more substituted ketones, are favored [20].

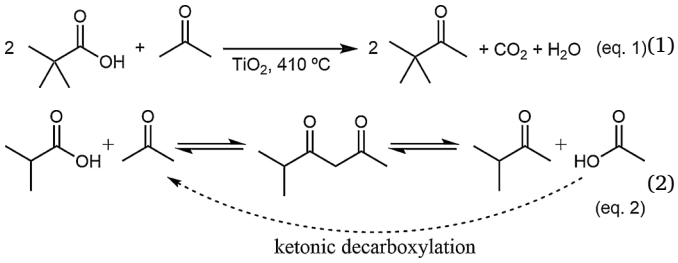

Taking into account the Green Chemistry principle, the reketonization is an outstanding reaction, provided that the ketonic decarboxylation is also taking place under the reaction conditions. This is quite likely, since reaction conditions and catalyst are identical. Then, the spent reagent is reconverted into fresh reagent (dashed arrow, Eq. (2)), producing two innocuous by-products, namely one molecule of carbon dioxide and one of water.

Herein, we will compare the production of methyl ketones by ketonic decarboxylation with acetic acid and by reketonization with acetone by Green Chemistry metrics, namely by carbon efficiency and e-factor [21, 22]. We will show by isotopic labeling that the ketonic decarboxylation proceeds much faster than the reketonization reaction. Furthermore, we will identify by *operando* IR spectroscopy a low level of acetone adsorption on the surface, under reaction conditions, as a clear impediment to the reketonization reaction.

2. Materials and methods

2.1. Materials

Monoclinic zirconium oxide was obtained from ChemPur, Germany, as pellets with a surface area of 103–104 $m^2 g^{-1}$. Thermal treatment at 650 °C and 750 °C for 6 h (heating rate 3 K/min) provided samples with surface areas of 53.4 m^2/g and 35.4 m^2/g, respectively [23]. XRD measurements were performed by means of a PANalytical Cubix'Pro diffractometer equipped with an X'Celerator detector and automatic divergence and reception slits using Cu-Kα radiation (0.154056 nm). The mean size of the ordered (crystalline) domains (d) was estimated using the Scherrer equation. The equation can be written as $d=(0.9\lambda)/(\beta \cos\theta)$, where λ is the X-ray wavelength, β is the line broadening at half the maximum intensity (FWHM), after subtracting the instrumental line broadening, in radians, and θ is the Bragg angle [23]. Nitrogen physisorption isotherms were obtained using a Micromeritics ASAP 2420 analyzer. The metal oxide was out-gassed in vacuum at 400 °C for 12 h prior to the analysis. The Brunauer–Emmett–Teller (BET) method was used to calculate the surface area in the range of relative pressures between 0.01 and 0.20 Pa.

Titanium oxide was also received from ChemPur, Germany, as pellets with a surface area of 149 m^2/g. The X-ray diffraction pattern showed that the titanium oxide was crystallized as anatase phase and broad signals were in accordance with surface area measured by nitrogen adsorption (i.e., with the relatively small crystal size). For further information on this material see reference [24]. Cerium oxide was obtained from Aldrich with an average particle size of 43 nm and a BET surface area of 63 m^2/g. For further information on this material see reference [25].

2.2. Catalytic reactions

All reactions were carried out in a tubular fixed-bed continuous flow reactor. The set-up has been described in a previous work [26]. The catalyst (1.0 g) was employed as pellets of 0.4 to 0.6 mm, diluted with silicon carbide and a gentle nitrogen carrier gas flow applied during the reaction. The reagents were fed to the reactor by the means of syringe pumps in two different solutions. A solution of decanoic acid (25 wt%) in hexadecane was prepared and introduced with WHSV =4.29 h^{-1}. Acetic acid was diluted with water, either in a 3 : 1 ratio (wt/wt) or a 7 : 1 ratio (wt/wt), and placed in a second syringe pump. Acetone was diluted with water in a 7 : 1 (wt/wt) and also fed separately from the decanoic acid. At the reactor outlet the liquids were condensed with ice-bath cooling. On standing, the liquid separated into an organic phase (upper layer) and an aqueous phase (lower layer). The aqueous layer was supposed to contain only a very minor amount of product which was not considered for the product balance.

Labeled acetic acid was purchased from Aldrich with a ^{13}C content at the 2-position of 99%. For the reaction of labeled acetic acid and non-labeled acetone, the second feed was composed by acetone, acetic acid and water in a 9 : 1 : 3 ratio (wt/wt/wt) and introduced to the reactor at a rate of 8.4 mL/min.

2.3. IR experiments

Interaction with the catalyst surface has been studied by *in situ* FT-IR spectroscopy of adsorbed acetic acid and acetone. The Fourier transform infrared (FTIR) spectra were recorded at room temperature on a Nicolet Nexus FTIR 5700 spectrometer (Thermo Scientific) equipped with a DTGS KBr detector and an extended KBr beam splitter at a spectral resolution of 4 cm^{-1} accumulating 128 scans. The powdered samples were pressed into thin self-supporting pellets of around 10 mg/cm^2 and placed in a vacuum quartz cell equipped with KBr windows, where they underwent all activation and adsorption treatments. Before the measurements, the samples were activated at 723 K for 1.5 h under high

vacuum (p = ~10^{-6} mbar) and treated with oxygen (5 min and 22 min) at the same temperature. Known amounts of either acetic acid or acetone were further introduced in the infrared cell using increasing aliquots untill surface saturation was reached.

For the IR *operando* experiments, the catalyst powder was again pressed into a self supported pellet that was further inserted into an IR cell reactor. The so called sandwich cell was then connected to the gas manipulation apparatus, consisting of mass flow controllers and thermoregulated saturator filled with liquid acetic acid. The reaction conditions were set to a total flow rate of 8 mL/min with an acetic acid molar fraction of 3%. The reaction was studied under a heating program specified in Fig. S5b. In addition, an IR gas cell (Thermo Scientific Nicolet iS50 GC-IR) allowed the analysis of the gaseous phase leaving the reactor. Infrared spectra (32 scans per spectrum) of both the catalyst and the gas phase were recorded alternately with an acquisition frequency of one spectrum every 87 s by means of a Thermo Scientific Nicolet iS50 FT-IR equipped with an MCT detector.

3. Results and discussion

3.1. Evaluation of the synthesis of methyl ketones by Green Chemistry metrics

The formation of methyl ketones starting from the carboxylic acid and either acetic acid or acetone should be evaluated employing Green Chemistry metrics, namely by the carbon (atom) efficiency and the environmental e-factor [27,28]. Atom efficiency (including hetero atoms) may be considered a less suitable metric for this reaction because elimination of oxygen, and therewith loss of certain classes of atoms, is desired and welcome in biorefinery. In this evaluation, the main question to be answered is whether the reketonization may outperform the classical ketonic decarboxylation from the ecological point of view under industrially relevant conditions.

The ketonic decarboxylation of carboxylic acid mixtures is a well-studied transformation for mixtures. Standard conditions with *monoclinic* zirconia were employed to set the benchmark for the reketonization. Water was used as co-feed in two different concentration as it has been observed that it can successfully suppress the aldol condensation reaction [29] that may occur in parallel and consume the acetone.

In a fixed-bed continuous-flow reactor two feeds were introduced in parallel, an organic one with decanoic acid (25 wt%) in hexadecane and an aqueous one containing acetic acid and water in a 7 : 1 (wt/wt) or a 3 : 1 (wt/wt) ratio. The feed rates were set at WHSV = 4.29 h^{-1} and WHSV = 8.90 h^{-1} for the organic and aqueous one, respectively, to achieve a 1 : 18 M ratio of decanoic acid and acetic acid. It was found that at a reaction temperature of 400 °C, both, acetic acid and decanoic acid were converted completely. From Fig. 1a and Scheme 1, it can be seen that the 2-undecanone desired product was obtained with 85 to almost 90% selectivity in the organic liquid product. Further products were 10-nonadecanone, 2-nonanone, 3,5-dimethyl-1-nonyl-benzene and 1,3-dinonyl-5-methyl-benzene. One molecule of acetic acid is incorporated into the 2-undecanone desired product. However, most of the acetic acid is converted into acetone. The latter is produced with 90% selectivity in the organic liquid (with respect to the acetic acid as starting material; Fig. 1b and Scheme 1).

Although the selectivity towards 2-undecanone in the liquid was good, the mass balance for the liquid itself was only moderate with 84 and 75% for 3 : 1 and 7 : 1 acetic acid to water ratios, respectively, after accounting for the noncondensable CO_2 gas loss (Table S1). This might be due to inefficient condensation of low weight products in the nitrogen flow such as water, acetone, etc. In addition, methane might be produced from acetic acid or acetone since the former has been observed when submitting a mixture of acid and ketone to the reaction conditions [30]. Hence, taking into account decanoic acid as starting material and 2-undecanone as product the carbon efficiency was 79% (with a 3:1 acetic acid/water ratio; see Table S1, Suppl. Data). However, this carbon efficiency is not meaningful, since the acetic acid reactant is not considered.

The carbon efficiency for the transformation of acetic acid into acetone is already limited by stoichiometry to 75% since one carbon atom out of four is transformed into carbon dioxide that has to be considered as a loss. Side product formation and non-quantitative mass balance lowered the carbon efficiency to the 50–60% range (Table S1, Suppl. Data). When taking into account both carboxylic acids and both ketones, the carbon efficiency was 62% (Table S1, Suppl. Data). This is the most reasonable value for the carbon efficiency of the reaction, provided that acetone is valorized as solvent or in other applications.

The second measurand, i.e., the e-factor, was calculated as the quotient of the sum of by-products and the mass of produced product (Table S2, Suppl. Data). When considering 2-undecanone as the only product, the e-factor was 11–13. Valorizing acetone lowers the e-factor to below 10 and considering a 90%-recovery of the solvent provides an e-factor below 5 (Table S2, Suppl. Data). The latter value makes the procedure suitable for bulk-chemical industry since in this respect, an e-factor of 5 is the upper limit. This means that, from the ecological point of view, it is reasonable to produce 2-undecanone on the multi-ton scale by the cross-ketonization of decanoic acid with an excess of acetic acid.

The alternative procedure selected for the production of 2-undecanone utilizes a reketonization reaction of acetone with decanoic acid [19,20]. Apart from the zirconia employed in the cross-ketonization above, two further standard commercial catalysts were chosen, namely titania (anatase) and ceria. The latter two are also well known for good performance in the ketonic decarboxylation of carboxylic acids [31,32]. From Scheme 2 it can be seen that all three materials catalyze the formation of the desired 2-undecanone. However, in all cases it is only the minor product. For ceria and zirconia, the 10-nonadecanone homo-coupling product was observed in almost 85% and 2-undecanone only in approximately 15% yield. Titania performed a bit better producing the desired ketone in 33 to 36% selectivity and the long-chain ketone with only 45% selectivity.

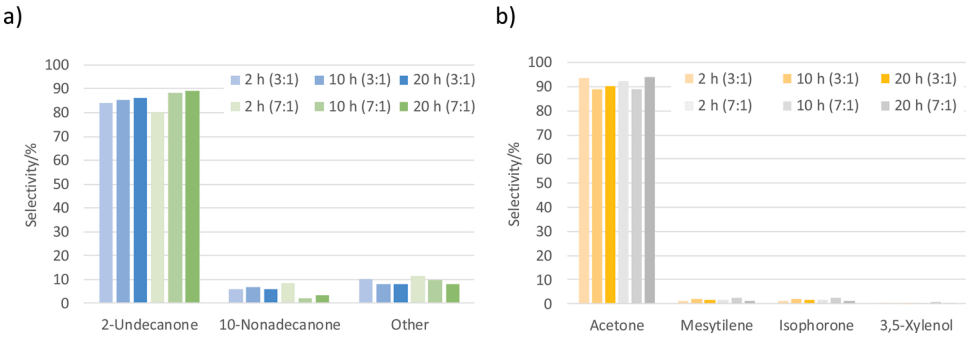

Fig. 1. Selectivities in the organic liquid for products derived from a) decanoic acid and b) acetic acid. The reaction was carried out in a fixed-bed continuous-flow reactor and the times refer to time on stream and the ratios, i.e, 3 : 1 and 7 : 1, to the acetic acid to water ratios (wt/wt) in the aqueous feed.

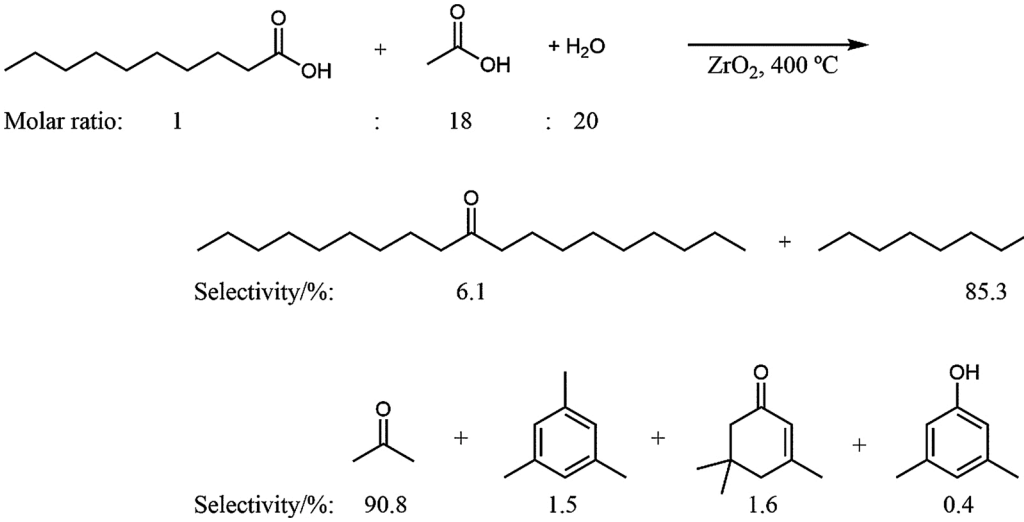

Scheme 1. Ketonic decarboxylation of decanoic acid with acetic acid in a 1 : 18 M ratio. Selectivities for 2-undecanone and 10-nonadecanone in the organic liquid were calculated based on decanoic acid as starting material and the selectivities for acetone, mesitylene, dimedone and 3,5-dimethylphenol from acetic acid.

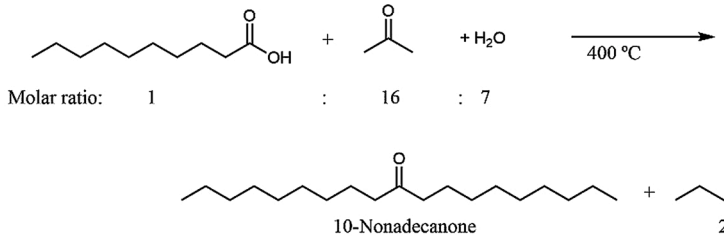

Catalyst	m^2/g	10-Nonadecanone [%]	2-Undecanone (2 h) [%]	Acetone conversion [%]
TiO_2	149	45	36 (33)	46
ZrO_2	103	83	14 (29)	29
CeO_2	61	84	15 (16)	27

Scheme 2. Reketonization of acetone with decanoic acid in a 16 : 1 M ratio. Selectivities for 2-undecanone and 10-nonadecanone in the organic liquid were calculated from decanoic acid after 10 h time on stream. Values in parenthesis for 2-undecanone refer to selectivities after 2 h time on stream.

Due to the low selectivity observed with all three catalysts, carbon efficiency was low and the e-factor was high. The exact values were not calculated since they were considered to be of preliminary nature. Catalytic performance towards the desired product has to be improved prior to a realistic evaluation of the transformation from the ecological point of view. Further efforts were made to reveal the mechanism on molecular scale and to identify the bottleneck of the reketonization. Therefore, the reketonization was studied by isotopic labeling. From the results above, it seemed that the ketonic decarboxylation was by far faster than the reketonization reaction and that this could be the reason for the unfavorable selectivity.

3.2. Isotopic labeling experiments

With the aim to estimate the relative reaction rates for ketonic decarboxylation and reketonization, an experiment involving acetic acid, isotopically labeled with carbon-13 in 2-position, and non-labeled acetone was performed (Scheme 3). From this mixture, two different 2-undecanone derivatives can be expected, the 1-^{13}C ketone, with the molecular ion detected by mass spectrometry as *m/z* 171, prepared from the reaction of decanoic acid with acetic acid and the unlabeled one, *m/z* 170, from the reaction of decanoic acid with acetone.

Monoclinic zirconia was selected as catalyst and 400 °C as reaction temperature. Under these conditions, the conversion of decanoic acid was complete. In the product mixture, 2-undecanone was observed in a

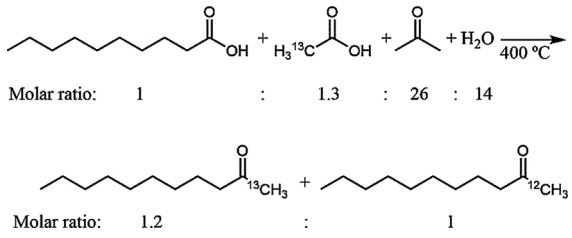

Scheme 3. Formation of 2-undecanone from decanoic acid with ^{13}C-labeled acetic acid or non-labeled acetone. Isotope distribution for 2-undecanone was determined by GC–MS. For more details on the calculation, see Suppl. Data.

1.2 : 1 mixture of the labeled and the non-labeled derivative (Fig. S1, Suppl. Data). The high percentage of the labeled atom incorporation showed that an unexpectedly large portion of 2-undecanone was obtained from the acetic acid relative to that from acetone, despite the fact that acetone was employed in the 20-fold excess. This result clearly confirms the direct incorporation pathway via cross-coupling ketonic decarboxylation instead of some hypothetical indirect incorporation.

The mechanism for the formation of ketones from the above mixture is shown in Scheme 4. There are two reaction pathways consuming the enolized acetone (Scheme 4a), one leading to the formation of unlabeled 2-undecanone, *m/z* 170, while the other one is a degenerate reaction

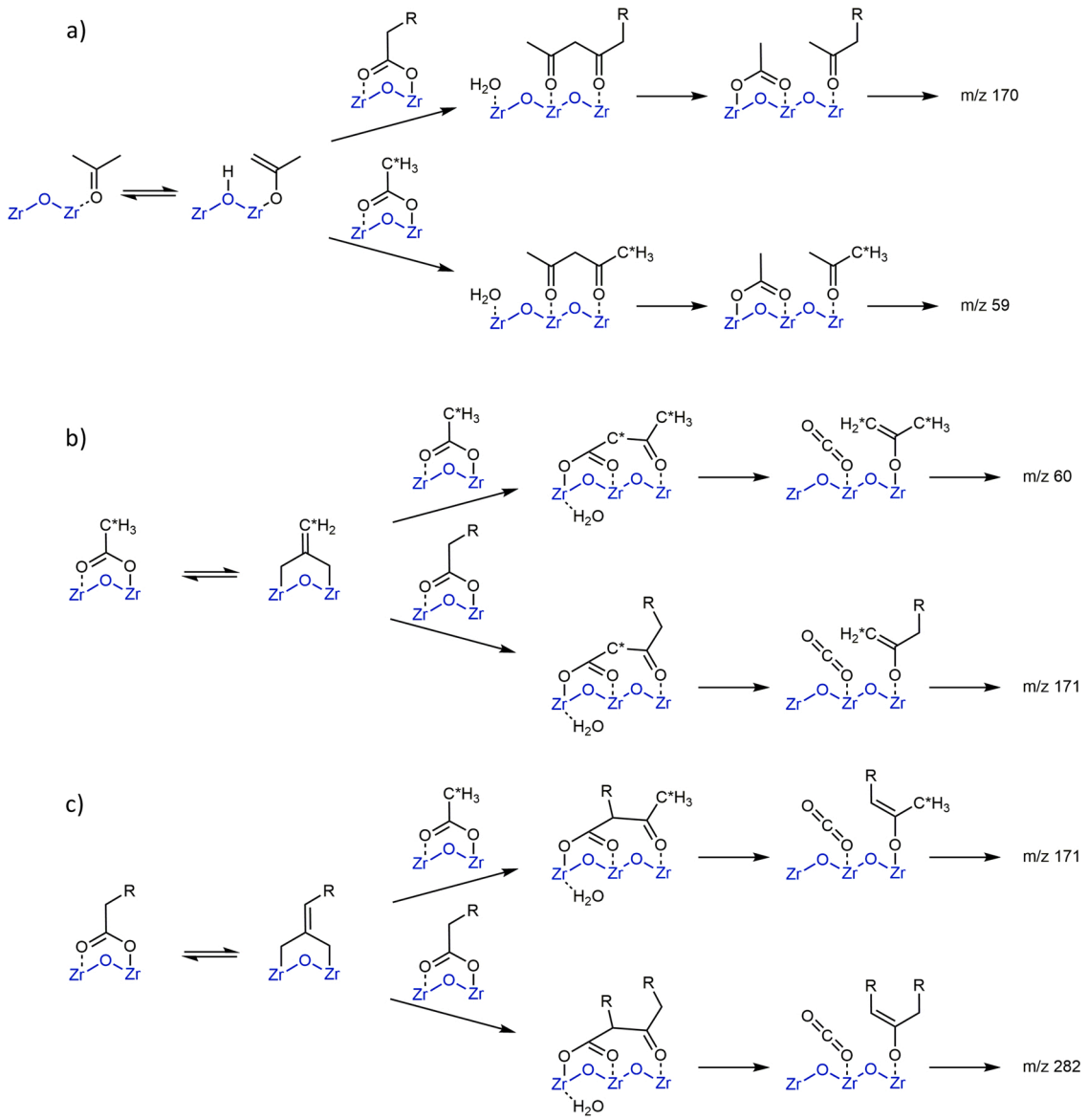

Scheme 4. Catalytic pathways to the formation of ketones: a) enolization of acetone and its condensation with decanoic acid yielding unlabeled 2-undecanone and a competing degenerate reaction of acetone with acetic acid leading to the scrambling of 13-C label, b) enolization of acetic acid followed by its condensation with itself and with decanoic acid leading to the formation of doubly labeled acetone and labeled 2-undecanone, respectively, and c) enolization of decanoic acid and its condensation with acetic acid and with itself providing another path to the labeled 2-undecanone and to 10-nonadecanone.

with acetic acid leading to the label scrambling and formation of acetone with the molecular ion *m/z* 59. At the same time, two pathways can lead to the formation of the labeled 2-undecanone, *m/z* 171, starting from the adsorption on surface and enolization of either acetic (Scheme 4b) or decanoic acid (Scheme 4c). Assuming that all three reagents, two carboxylic acids and acetone, compete for the same catalytic sites on surface, the molar ratio of decanoic acid : acetic acid : acetone = 1 : 1 : 1 should provide 2-undecanone molecular ions *m/z* 171 : *m/z* 170 in the 2 : 1 ratio on a purely statistical basis. For the applied ratio of reagents, 1 : 1.3 : 26, the statistically expected ratio of *m/z* 171 : *m/z* 170 is 1 : 10 (for details see Suppl. Data). However, the actual experimental result is different by a factor of 12 (1.2 vs. 0.1) which can be attributed to the difference between the rates of the three competing reaction pathways, two of which are condensations between decanoic acid and acetic acid, while the third one is acetone condensation with decanoic acid. It could be due to the difference in the reaction rate constants of the rate limiting condensation step, or due to the concentration of the three enolized species on the active sites. Because alpha protons in ketones are more acidic compared to that in carboxylates, the difference in the concentration of the enolized species must be explained by a weaker adsorption of acetone compared to carboxylic acids.

Decarboxylative condensation of acetic acid with itself produced acetone isotopologue with two ^{13}-C labels, *m/z* 60, which was blended with the starting acetone, *m/z* 58, and with another isotopologue, *m/z* 59, providing the statistical ratio of labeled atoms in the methyl groups below 5% (Fig. S1). The by-products derived from side reactions of the mixture of acetone isotopologues, such as mesityl oxide or isophorone, had the same distribution of the 13-C label. Therefore, the post-distribution of the 13-C label and its incorporation into 2-undecanone could not exceed 5% for statistical reasons.

In conclusion, the isotopic labeling experiments confirm unambiguously that the ketonic decarboxylation reaction of decanoic acid with acetic acid is significantly faster under reaction conditions than the reketonization of the same carboxylic acid with acetone.

3.3. In-situ IR spectroscopy for adsorption/desorption sequences of acetic acid and acetone

The DFT calculations revealed an adsorption energy of −193 kJ/mol for acetic acid onto the zirconia surface and less than half of this value for acetone desorption, namely 84 kJ/mol [33]. These values indicate that acetic acid should be adsorbed preferentially compared to acetone and that the surface should be covered by the acid during the reaction. Indeed, from the above values and assuming similar adsorption entropies for acetic acid and acetone, it can be estimated from the Eq. (3)

$$e^{\left(\frac{\Delta H_{ads,\ acetone} - \Delta H_{ads,\ acid}}{RT}\right)} \quad (3)$$

that a surface ratio $\frac{acetic\ acid_{ads}}{acetone_{ads}}$ of about 2.9 10^8 would be reached when submitting the catalyst to similar reactant partial pressure. The lack of adsorbed acetone on the surface may thus be one reason for the moderate performance of the reketonization reaction with respect to the ketonic decarboxylation. With the aim to support the theoretical data and this hypothesis, *in-situ* and *operando* FT-IR spectroscopic experiments were carried out.

Zirconia was pressed into a self-supported wafer and placed in an *in-situ* IR cell [34]. After catalyst pre-treatment and evacuation of the cell, acetic acid was admitted to the cell successively in small amounts at room temperature. After each addition, an IR spectrum was recorded of the surface. From Fig. 2a it can be seen that the aliquots are adsorbed onto the surface and that all bands are growing constantly in the region of 2000 to 800 cm^{-1}. The main shape is a doublet with the maxima at 1552 cm^{-1} and 1459 cm^{-1}, and with shoulders at 1424 cm^{-1} and 1386 cm^{-1}. The two most intense peaks are tentatively assigned to νa (OCO) and νs (OCO) of adsorbed acetates [35–37], most probably as bidentate species [38]. No new bands were observed until surface saturation revealed by the appearance of physisorbed acetic acid, indicated by the band at 1712 cm^{-1}.

Interestingly, a very similar behavior was observed when zirconia samples with BET surface areas of 53 or 35 m^2/g were employed (Fig. S2, Suppl. Data) instead of the sample with a BET surface area of 100 m^2/g. Bands were observed at the same wavenumbers and the composed signal had a very similar shape (Fig. S2c, Suppl. Data). The sample with higher surface area had a smaller average crystal size and, therefore, a higher ratio of active sites at corners and edges with respect to planar surface sites [23]. When no difference is observed for different ratios of sites, it can be concluded that the adsorption mode is little influenced by the surface geometry of the catalyst material, i.e., there is no preference for the adsorption at the edges.

DFT calculations were carried out placing two acetic acid molecules on a 111 zirconia surface. The intensities of the different vibration modes are depicted in Fig. 3. Considering a redshift of approximately 30 cm^{-1} to lower wavenumbers (with respect to the experimental data), the shape of the composed spectrum (with a broader peak width) resembles the experimental one. Therefore, this study further corroborates a bidentate coordination mode to two different zirconium atoms, even with acetate molecules in the neighborhood. In contrast, when the same study is done for the $1\bar{1}1$ zirconia surface the match is not evident (Fig. S3). This is explained by a mismatch of the surface plane, but no experimental support can be provided for this argument.

The successive adsorption procedure in the *in-situ* IR spectroscopy experiment was repeated with acetone and a fresh zirconia sample with a BET surface area of 100 m^2/g (Fig. 2b). Three major signal ranges were observed: from 1730 to 1525 cm^{-1} with two maxima at 1680 and 1600 cm^{-1}, from 1395 to 1340 cm^{-1}, and from 1270 to 1150 cm^{-1}, with three maxima at 1250, 1223, and 1170 cm^{-1}. The last range is suitable to distinguish between adsorbed acetone and adsorbed acetic acid, and to confirm the presence of acetone on a surface covered with an excess of acetic acid, since the spectrum of adsorbed acetic acid does not involve any band in this region (Fig. 2c). Vice versa, the band at a wavenumber of 1552 cm^{-1} is indicative for acetic acid, which exhibits a strong intensity (as part of a doublet), whereas the signal of acetone consists of a smooth decline without any shoulder.

In conclusion, *in-situ* IR spectroscopy of acetic acid and acetone adsorbed onto a zirconia surface demonstrated that both compounds are unambiguously distinguishable by this method. Therefore, IR spectroscopy is a method of choice to study the ketonic decarboxylation of acetic

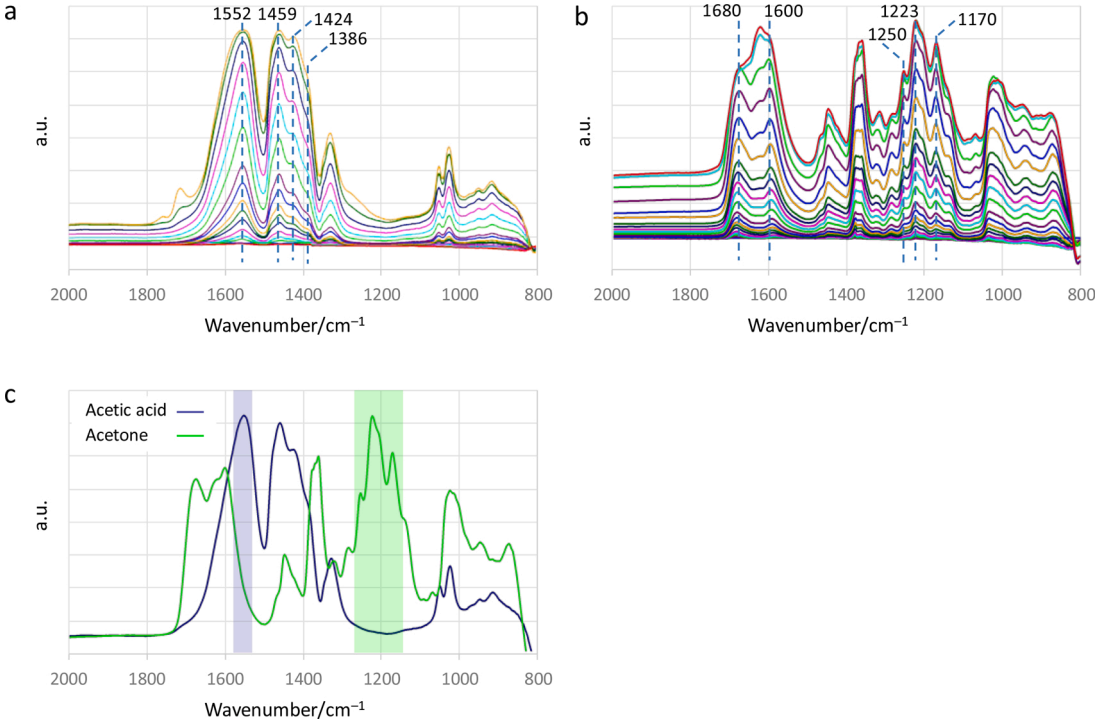

Fig. 2. *In situ* IR-spectra of a) acetic acid and b) acetone adsorbed successively onto the zirconia waver with a BET surface area or 104 m^2/g, and c) of both compounds at high surface saturation.

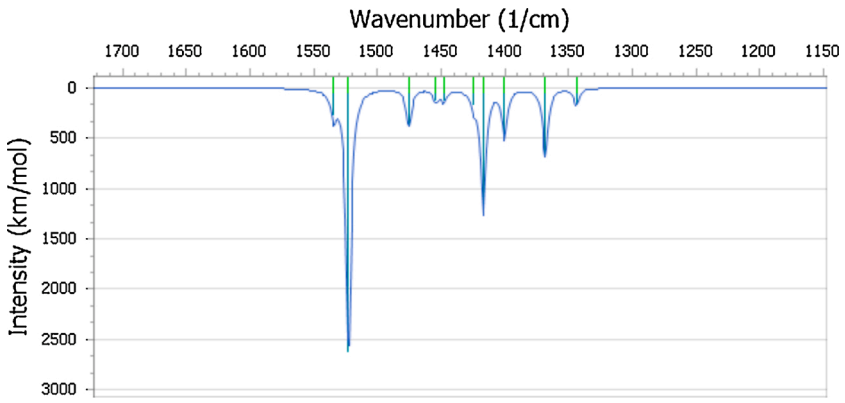

Fig. 3. Composite spectrum of the IR simulated vibrations obtained by the previously described DFT method [39] for a model which includes two acetate molecules and two protons adsorbed on 111 surface of monoclinic zirconia (Wavenumbers and relative intensities are listed in Table S3 and vibration modes are depicted in Figure S4).

acid and the reketonization of acetic acid with acetone in *operando* conditions.

3.4. Operando IR spectroscopy for the ketonic decarboxylation of acetic acid to acetone

3.4.1. Influence of the temperature on the signal shape

For the FTIR *operando* experiment, a zirconia (BET surface area of 100 m^2/g) wafer was placed in an *operando* IR reaction chamber [40]. An acetic acid stream was passed through the chamber and the gas effluent was also monitored by IR spectroscopy. The complete experiment is depicted in a 3D image in Fig. S5a with the corresponding temperature profile in Fig. S5b. Temperature was raised successively from 215 °C to 315, 338, 363, 387 and 411 °C (Fig. S5b). Fig. S6 shows a 2D image of the same experiment.

From the Figs. S5a and S6a is can be seen that the surface is immediately covered and only minor changes occur during the first 100 min on stream. In Fig. 4a a comparison is shown between a spectrum recorded at 215 °C under *operando* conditions and one of adsorbed acetic acid recorded at room temperature under *in-situ* conditions. Both spectra show the same bands. Additional bands were not observed in either one of them. Therefore, it can be concluded that at 215 °C the surface of zirconia is only covered by acetic acid mostly as acetates.

From the 2D image (Fig. S6a) it seems that the νs (OCO) bands for adsorbed acetates broaden after 30 min on stream, that is when starting to increase the temperature from 215 to 315 °C. For a better understanding of the occurrence, single spectra recorded at different temperatures, i.e., at 215, 315, 338, and 363 °C were selected and presented in Fig. 4a. From this illustration, it becomes evident that the signal suffers a change: when increasing temperature the two shoulders at a wavenumber of approximately 1400 cm^{-1} disappear (Fig. 4a). This can be seen even better in Fig. 4b, in which the signal is compared for the temperatures of 215 and 387 °C. The doublet signal becomes symmetrical at higher temperature and, therewith a bit broader towards lower wavenumbers (Fig. 4b). This is the reason for the widening of the right red line after 30 min in Fig. S6a.

Several hypothesis for the reason for the change in the signal shape can be taken into account. If the shoulders are due to different vibration modes, as the DFT study suggests, then the increase of the temperature should cause a variation in the intensities for these modes. If the shoulders are due to different species, e.g., with slightly different geometry or activation, these species may be more reactive. As a consequence, they are converted first and the corresponding sites are unoccupied. However, experimental support could not be found for either one of the two hypotheses.

3.4.2. Influence of the temperature on the reaction outcome at constant flow

The exhaust flow from the reaction chamber was monitored by IR spectroscopy and the spectra are depicted as 2D image in Fig. S6b. For the interpretation of the experiment, it has to be taken into account that carboxylic acids, when increasing their concentration in the gas phase, aggregate and form dimers. At very low concentration, the molecules are present as monomers.

This concentration-dependent monomer-dimer equilibrium in the gas-phase has an influence on the IR interpretation since both species have different IR spectra, i.e., they can be differentiated by IR spectroscopy. Fig. S7 depicts the IR spectra of acetic acid in the gas phase, in Fig. S7a at increasing concentration and in Fig. S7b comparing the spectra for the lowest and the highest concentrations (of the series) with

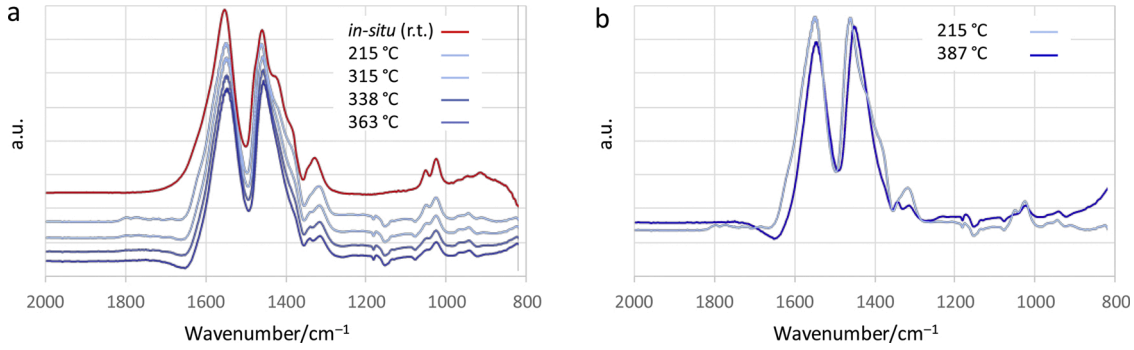

Fig. 4. a) *operando* IR-spectra of the surface of *monoclinic* zirconia (BET surface area or 104 m^2/g) when passing acetic acid a) at increasing temperature, compared with the *in-situ* spectrum of acetic acid adsorbed onto the same material and recorded at room temperature; b) comparison of two *operando* IR-spectra recorded at different temperature.

the same height of the strongest band.

At higher concentration (dark purple line), the spectrum is characterized by two sharp single bands at wavenumbers of 1734 and 1294 cm^{-1} (Fig. S7b). These two bands are assigned to the ν(C═O) and ν(C–O) modes for the acetic acid dimer respectively [41]. At lower concentration (dark green line), peaks already present in the former spectrum become more relevant, namely at 1790 and 1180 cm^{-1}. The latter two are characteristic for the monomer species of acetic acid in the gas phase.

The comparison of the IR spectra of the gas phase involving a low acetic acid concentration and of the gas phase of the exhaust gas after passing acetic acid over zirconia at 215 °C revealed that both are very similar and the major bands are identical (Fig. S8). Therefore, it can be concluded that when passing acetic acid at 215 °C no chemical transformation takes place. The surface coverage is maximum and excess acetic acid leaves the reactor chamber without catalytic conversion.

When having a closer look on Fig. S6b at the zone of the first temperature increase (30 to 50 min), it becomes evident that a change occurs at a temperature of approximately 260 °C (marked with a dashed line). The single spectra of this range from 265 to 315 °C are depicted in Fig. 5. The acetic acid bands started to fade in the reactor effluent, whereas new bands appeared at wavenumbers of 2400 cm^{-1}. The latter are characteristic for carbon dioxide. Hence, this temperature range was considered as that at which the reaction initiates. This is in accordance with the observation that in a pulse reactor coupled with mass spectrometry, the ketonic decarboxylation started already at a temperature as low as 180 °C [42]. The other IR peaks position remain similar to what was detected in the lower temperature range while their intensity ratio changed: the proportion of monomeric acetic acid increased which is consistent with both a lowering of the CH_3COOH concentration (being partly converted to CO_2) and an increase of the reaction temperature favoring the dimer dissociation.

After 70 min, the period of change in the product mixture ended: no more acetic acid was detected, i.e., the conversion was complete. This can be seen in the two-dimensional image (Fig. S6b) and the transformation of the product composition can be tracked in Fig. 6 based on several selected spectra. When comparing the spectra at full conversion, i.e., for the temperature range from 363 to 411 °C (75 to 130 min), with the spectrum of acetone and the one of a mixture of carbon dioxide and water, it was confirmed that these three compounds are the sole products of acetic acid conversion (Fig. 7).

The analysis of the gas phase proved unambiguously the formation and the presence of acetone. However, when going back to the surface (Fig. S6a), no evidence at all was found for adsorbed acetone onto the surface. As discussed above, a signal at wavenumbers of 1200 cm^{-1} should arise (Fig. 2). This is clearly not the case. When reaching 387 and 411 °C, the coverage with acetic acid decreased (Fig. S6a). However, no new signals arose. This was a clear proof for the hypothesis that the adsorption of acetone at temperatures around 400 °C was not favored, although the surface was not fully covered by acetic acid. Hence, if the residence time of the acetone on the surface was short, reketonization was disfavored, whereas ketonic decarboxylation can proceed smoothly due to the presence of plenty of carboxylic acid.

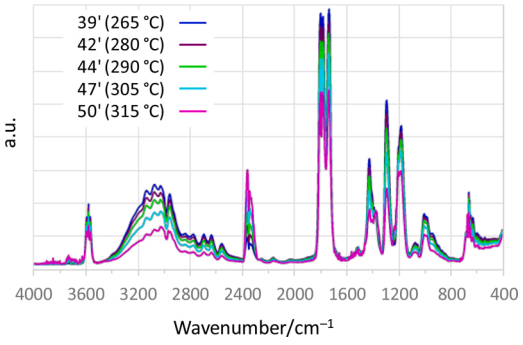

Fig. 5. Gas-phase IR-spectra after passing acetic acid over monoclinic zirconia at increasing temperature in the range from 265 to 315 °C.

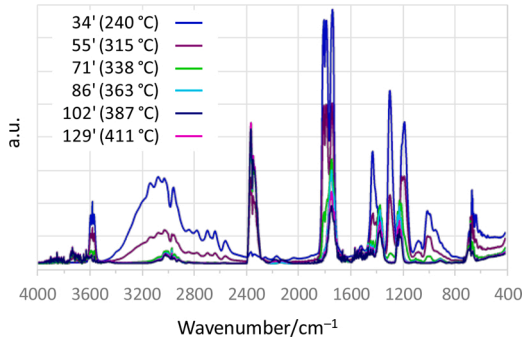

Fig. 6. Gas-phase IR-spectra after passing acetic acid over monoclinic zirconia at increasing temperature in the range from 265 to 411 °C.

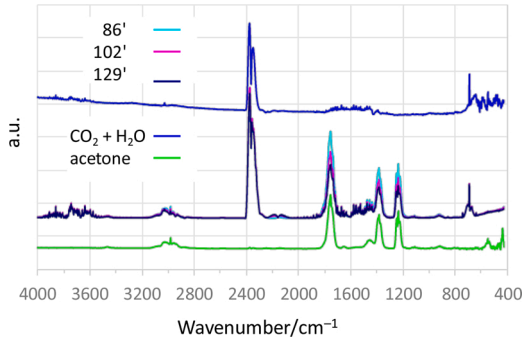

Fig. 7. Gas-phase IR-spectra after passing acetic acid over monoclinic zirconia at increasing temperature in the range from 265 to 411 °C.

4. Conclusions

The synthesis of methyl ketones was targeted from carboxylic acids without metalorganic reagents. When employing decanoic acid as model compound, 2-undecanone was obtained either by cross-coupling ketonic decarboxylation with acetic acid or by reketonization with acetone. However, fundamental differences were observed when the transformations were evaluated for their sustainability.

The cross-coupling ketonic decarboxylation provided an e-factor below five, which is acceptable for production even as a bulk chemical. In contrast, for the reketonization of decanoic acid with acetone, the 10-nonadecanone ketonization product was always obtained as main product. This frustrated any positive evaluation when 10-nonadecanone was considered as an undesired product.

The relative reaction rate of both transformations was studied by an isotopic labeling experiment. Acetic acid with a ^{13}C-carbon atom in 2-position was reacted with decanoic acid in presence of 20-fold excess of acetone. Nevertheless, approximately the same amounts of labeled and unlabeled methyl groups were detected in the 2-undecanone product. This indicated that the ketonic decarboxylation was significantly faster than the reketonization.

It was hypothesized that the reason for the lower rate was the low concentration of acetone on the surface and *in-situ* and *operando* IR experiments were carried out. It was shown that indeed the surface was covered by acetic acid, whereas adsorbed acetone was not detected under reaction conditions, i.e., at 400 °C, although the coverage of the surface by acetic acid was not complete at this temperature and gaseous acetone was produced. The above results thus confirm that the reketonization reaction is limited by the absence of acetone activation through

adsorption and that consequently the reketonization reaction would take place through a Langmuir Hinshelwood mechanism involving both adsorbed acid and adsorbed ketone.

In order to improve the performance of the reketonization, catalyst properties should thus be modified to improve the adsorption of acetone along with carboxylic acids.

CRediT authorship contribution statement

Olivier Marie: Writing - review & editing. **Alexey V. Ignatchenko:** Writing - review & editing. **Michael Renz:** Conceptualization, Supervision.

Declaration of Competing Interest

The authors declare that they have no known competing financial interests or personal relationships that could have appeared to influence the work reported in this paper.

Acknowledgements

Financial support from the Spanish Government is acknowledged (Ministry of Science, Innovation and Universities, RTC-2017-6087-5 and PGC2018-097277-B-I00). MR is grateful to the Generalitat Valenciana for a BEST-2015 fellowship and to Dilyana Mladenova, Arturo Valero Jiménez and Claudia Fernández de la Peña for their contributions to the experimental work of the catalytic reactions.

Appendix A. Supplementary data

Supplementary material related to this article can be found, in the online version, at doi:https://doi.org/10.1016/j.cattod.2020.03.042.

References

[1] Ketone brochure, Shell Chemicals, 2011. https://www.shell.com/business-customers/chemicals/our-products/solvents-chemical/ketones/methyl-isobutyl-ketone-mibk/_jcr_content/par/tabbedcontent/tab/textimage.stream/1519786997308/ab988544d68103fc94b1421be4d58dfc468a7ca4/ketones-brochuredec2011.pdf.

[2] Product catalogue, Firmenich, 2016. https://www.firmenich.com/uploads/files/ingredients/Compendium_Flavors_Ingredients_2016.pdf.

[3] H.S. Whang, A. Tonelli, Release characteristics of the non-toxic insect repellant 2-undecanone from its crystalline inclusion compound with α-cyclodextrin, J. Incl. Phenom. Macrocycl. Chem. 62 (2008) 127–134, https://doi.org/10.1007/s10847-008-9447-z.

[4] G.S. Pirro Rafael, Use of 2-undecanone for manufacturing animal-repellent trash bags, Costa Rica Patent Application *CR7082A*, 2008.

[5] L. Kensek, W.L. Mateo, Concentrated Composition for Insect and Animal Control Containing Methyl Nonyl Ketone, US Patent Application *US20030086955A1*, 2003.

[6] L.H.J. Kleijn, S.F. Oppedijk, P. 't Hart, R.M. van Harten, L.A. Martin-Visscher, J. Kemmink, E. Breukink, N.I. Martin, Total synthesis of laspartomycin C and characterization of its antibacterial mechanism of action, J. Med. Chem. 59 (2016) 3569–3574, https://doi.org/10.1021/acs.jmedchem.6b00219.

[7] B.B. Damaj, R.M. Martin, Preparation of Antimicrobial Compounds and Methods of Use, PCT Int. Application *WO2014093252A1*, 2014.

[8] M.B. Richardson, S.J. Williams, A practical synthesis of long-chain iso-fatty acids (iso-C12-C19) and related natural products, Beilstein Journal of Nanotechnology 9 (2013) 1807–1812, https://doi.org/10.3762/bjoc.9.210, 6 pp.

[9] B.L. Merner, K.S. Unikela, L.N. Dawe, D.W. Thompson, G.J. Bodwell, 1,1,n,n-tetramethyl[n](2,11)teropyrenophanes (n = 7-9): a series of armchair SWCNT segments, Chem. Commun. (Camb. United Kingd.) 49 (2013) 5930–5932, https://doi.org/10.1039/c3cc43268h.

[10] S. Saveliev, D. Simpson, K.V. Wood, Cleavable Surfactants PCT Int. Application *WO2009048611A2* 2009.

[11] N.A. Porter, V.H.T. Chang, Macrolide formation by free radical cyclization, J. Am. Chem. Soc. 109 (1987) 4976–4981, https://doi.org/10.1021/ja00250a036.

[12] R. Senatore, L. Ielo, S. Monticelli, L. Castoldi, V. Pace, Weinreb amides as privileged acylating agents for accessing α-substituted ketones, Synthesis (Stuttg). 51 (2019) 2792–2808, https://doi.org/10.1055/s-0037-1611549.

[13] M. Nowak, Weinreb Amides, Synlett. 26 (2015) 561–562, https://doi.org/10.1055/s-0034-1380055.

[14] S. Balasubramaniam, I.S. Aidhen, The growing synthetic utility of the weinreb amide, Synthesis (Stuttg) (2008) 3707–3738, https://doi.org/10.1055/s-0028-1083226.

[15] V.K. Khlestkin, D.G. Mazhukin, Recent advances in the application of N,O-dialkylhydroxylamines in organic chemistry, Curr. Org. Chem. 7 (2003) 967–993, https://doi.org/10.2174/1385272033486639.

[16] M. Mentzel, H.M.R. Hoffmann, N-methoxy N-methyl amides (weinreb amides) in modern organic synthesis, J. Fuer Prakt. Chemie/Chemiker-Zeitung. 339 (1997) 517–524, https://doi.org/10.1002/prac.19973390194.

[17] M. Renz, Ketonization of carboxylic acids by decarboxylation: mechanism and scope, European J. Org. Chem. (2005) (2005) 979–988, https://doi.org/10.1002/ejoc.200400546.

[18] A.V. Ignatchenko, J.S. DeRaddo, V.J. Marino, A. Mercado, Cross-selectivity in the catalytic ketonization of carboxylic acids, Appl. Catal. A Gen. 498 (2015) 10–24, https://doi.org/10.1016/j.apcata.2015.03.017.

[19] C. Schommer, K. Ebel, T. Dockner, M. Irgang, W. Hoelderich, H. Rust, Verfahren zur Herstellung von Ketonen, EP0352674B1 (1989).

[20] A.V. Ignatchenko, T.J. DiProspero, H. Patel, J.R. LaPenna, Equilibrium in the catalytic condensation of carboxylic acids with methyl ketones to 1,3-diketones and the origin of the reketonization effect, ACS Omega. 4 (2019) 11032–11043, https://doi.org/10.1021/acsomega.9b01188.

[21] R.A. Sheldon, Metrics of Green chemistry and sustainability: past, present, and future, ACS Sustain. Chem. Eng. 6 (2018) 32–48, https://doi.org/10.1021/acssuschemeng.7b03505.

[22] D.J.C. Constable, A.D. Curzons, V.L. Cunningham, Metrics to 'green' chemistry—which are the best? Green Chem. 4 (2002) 521–527, https://doi.org/10.1039/B206169B.

[23] B. Oliver-Tomas, F. Gonell, A. Pulido, M. Renz, M. Boronat, Effect of the Cα substitution on the ketonic decarboxylation of carboxylic acids over m-ZrO2: the role of entropy, Catal. Sci. Technol. 6 (2016) 5561–5566, https://doi.org/10.1039/C6CY00395H.

[24] B. Oliver-Tomas, M. Renz, A. Corma, Direct conversion of carboxylic acids (Cn) to alkenes (C2n−1) over titanium oxide in absence of noble metals, J. Mol. Catal.. A Chem. 415 (2016) 1–8, https://doi.org/10.1016/j.molcata.2016.01.019.

[25] L.M. Orozco, M. Renz, A. Corma, Cerium oxide as a catalyst for the ketonization of aldehydes: mechanistic insights and a convenient way to alkanes without the consumption of external hydrogen, Green Chem. 19 (2017) 1555–1569, https://doi.org/10.1039/C6GC03511F.

[26] A. Pulido, B. Oliver-Tomas, M. Renz, M. Boronat, A. Corma, Ketonic decarboxylation reaction mechanism: A combined experimental and DFT study, ChemSusChem. 6 (2013) 141–151. http://www.scopus.com/inward/record.url?eid=2-s2.0-84872293574&partnerID=40&md5=dc00fb85bba914d9d01e2d3ffbf2b95a.

[27] D.J.C. Constable, A.D. Curzons, V.L. Cunningham, Metrics to 'green' chemistry—which are the best? Green Chem. 4 (2002) 521–527, https://doi.org/10.1039/B206169B.

[28] R.A. Sheldon, Metrics of green chemistry and sustainability: past, present, and future, ACS Sustain. Chem. Eng. 6 (2018) 32–48, https://doi.org/10.1021/acssuschemeng.7b03505.

[29] L.M. Orozco, M. Renz, A. Corma, carbon-carbon bond formation and hydrogen production in the ketonization of aldehydes, ChemSusChem. 9 (2016) 2430–2442, https://doi.org/10.1002/cssc.201600654.

[30] S.D. Barnicki, D. McNabb, J.E. Ward, Process for reducing emissions of volatile organic compounds from the ketonization of carboxylic acids, US20130310608A1 (2013).

[31] S. Wang, E. Iglesia, Experimental and theoretical assessment of the mechanism and site requirements for ketonization of carboxylic acids on oxides, J. Catal. 345 (2017) 183–206, https://doi.org/10.1016/j.jcat.2016.11.006.

[32] A. Gangadharan, M. Shen, T. Sooknoi, D.E. Resasco, R.G. Mallinson, Condensation reactions of propanal over CexZr 1-xO2 mixed oxide catalysts, Appl. Catal. A Gen. 385 (2010) 80–91. http://www.scopus.com/inward/record.url?eid=2-s2.0-77956358169&partnerID=40&md5=2b2b9944d0dc8f5802fa73a08963cd69.

[33] A. Pulido, B. Oliver-Tomas, M. Renz, M. Boronat, A. Corma, Ketonic decarboxylation reaction mechanism: a combined experimental and DFT study, ChemSusChem. 6 (2013) 141–151, https://doi.org/10.1002/cssc.201200419.

[34] O. Marie, F. Thibault-Starzyk, P. Massiani, Conversion of xylene over mordenites: an operando infrared spectroscopy study of the effect of Na+, J. Catal. 230 (2005) 28–37, https://doi.org/10.1016/j.jcat.2004.09.023.

[35] J. Shibata, K. Shimizu, S. Satokawa, A. Satsuma, T. Hattori, Promotion effect of hydrogen on surface steps in SCR of NO by propane over alumina-based silver catalyst as examined by transient FT-IR, Phys. Chem. Chem. Phys. 5 (2003) 2154–2160, https://doi.org/10.1039/B302352D.

[36] J. Dupré, P. Bazin, O. Marie, M. Daturi, X. Jeandel, F. Meunier, Effects of temperature and rich-phase composition on the performance of a commercial NOx-storage-reduction material, Appl. Catal. B Environ. 181 (2016) 534–541, https://doi.org/10.1016/j.apcatb.2015.08.033.

[37] L.F. Bobadilla, O. Marie, P. Bazin, M. Daturi, Effect of Pd addition on the efficiency of a NOx-trap catalyst: A FTIR operando study, Catal. Today. 205 (2013) 24–33, https://doi.org/10.1016/j.cattod.2012.08.019.

[38] M.A. Hasan, M.I. Zaki, L. Pasupulety, Oxide-catalyzed conversion of acetic acid into acetone: an FTIR spectroscopic investigation, Appl. Catal. A Gen. 243 (2003) 81–92, https://doi.org/10.1016/S0926-860X(02)00539-2.

[39] A.V. Ignatchenko, J.P. McSally, M.D. Bishop, J. Zweigle, Ab initio study of the mechanism of carboxylic acids cross-ketonization on monoclinic zirconia via condensation to beta-keto acids followed by decarboxylation, Mol. Catal. 441 (2017) 35–62, https://doi.org/10.1016/j.mcat.2017.07.019.

[40] S. Thomas, O. Marie, P. Bazin, L. Lietti, C.G. Visconti, M. Corbetta, F. Manenti, M. Daturi, Modelling a reactor cell for operando IR studies: from qualitative to fully

quantitative kinetic investigations, Catal. Today. 283 (2017) 176–184, https://doi.org/10.1016/j.cattod.2016.07.008.
[41] J. Chocholoušová, J. Vacek, P. Hobza, acetic acid dimer in the gas phase, nonpolar solvent, microhydrated environment, and dilute and concentrated acetic acid: ab initio quantum chemical and molecular dynamics simulations, J. Phys. Chem. A. 107 (2003) 3086–3092, https://doi.org/10.1021/jp027637k.
[42] A.V. Ignatchenko, E.I. Kozliak, Distinguishing enolic and carbonyl components in the mechanism of carboxylic acid ketonization on monoclinic zirconia, ACS Catal. 2 (2012) 1555–1562, https://doi.org/10.1021/cs3002989.